Experimental investigations of one liquid-crystal compound exhibiting the no-layer-shrinkage effect near the Sm-*A*–Sm-*C** transition

C. C. Huang,[1] S. T. Wang,[1] X. F. Han,[1] A. Cady,[1,*] R. Pindak,[2] W. Caliebe,[2] K. Ema,[3] K. Takekoshi,[3] and H. Yao[3]
[1]*School of Physics and Astronomy, University of Minnesota, Minneapolis, Minnesota 55455, USA*
[2]*NSLS, Brookhaven National Laboratory, Upton, New York 11973, USA*
[3]*Department of Physics, Graduate School of Science and Engineering, Tokyo Institute of Technology, 2-12-1 Oh-okayama, Meguro, 152 Tokyo, Japan*
(Received 12 December 2003; published 16 April 2004)

Three experimental probes have been employed to investigate the nature of the smectic-*A*–smectic-*C* (Sm-*A*–Sm-*C**) phase transition of one liquid-crystal compound showing almost no layer-shrinkage effect through the transition. Results from both x-ray diffraction and optical studies indicate that the compound exhibits a crossover behavior of different molecular packing arrangements within the bulk Sm-*A* phase window. The calorimetry results show a significant critical anomaly near the Sm-*A*–Sm-*C** transition, although it was found to be weakly first order.

DOI: 10.1103/PhysRevE.69.041702 PACS number(s): 61.30.Eb, 64.70.−p, 64.60.Fr

Smectic-*A* (Sm-*A*) and smectic-*C* (Sm-*C*) are two important mesophases found in many rodlike liquid-crystal compounds. If the constituent molecules are chiral, the chiral smectic-*C* (Sm-*C**) phase forms instead of the Sm-*C* phase. To characterize the direction of the molecular long axes (denoted by the **n** director), we use two parameters: θ [tilt angle from the layer normal (**z**)] and ϕ (azimuthal angle). In the Sm-*C** phase, the chirality breaks the mirror symmetry in the tilt plane, defined by **z** and **n**, and allows the existence of a net electric dipole moment normal to the tilt plane [1]. Consequently, one of the prominent features associated with the Sm-*A*–Sm-*C** transition is the electroclinic effect in the Sm-*A* phase [2] in which the average tilt angle is directly related to an applied electric field (E). Recently, an unusually large electroclinic effect near the Sm-*A*–Sm-*C** transition of several liquid-crystal compounds has been reported [3–6]. This class of compounds also shows no-layer-shrinkage (NLS) behavior through the Sm-*A*–Sm-*C** transition. Both a large electroclinic effect and NLS behavior are extremely important in utilizing Sm-*C** material for electro-optical device applications. Thus, a considerable amount of attention has been aimed at understanding the origin of the molecular tilt in the Sm-*C* (or Sm-*C**) phase as well as the true molecular packing arrangement of this class of compounds. To date, at least two models have been proposed to explain the electroclinic effect. In the first, **n** is assumed to be parallel to **z** in the Sm-*A* phase. Under an applied electric field, the molecules tilt [2]. This results in a significant change in the smectic layer spacing. In the second approach suggested by de Vries *et al.* [7], the molecules in the Sm-*A* phase are assumed to be tilted through a finite angle θ_A in the absence of an applied electric field, but are spatially disordered in their azimuths. Specifically, the azimuthal distribution function is uniform, $f(\phi)=1/(2\pi)$, on a cone about **z**. Then an applied electric field in the layer plane promotes azimuthal order, without any significant change in θ_A or the smectic layer spacing. Small angle x-ray diffraction yields very different results between these two scenarios. Upon cooling through the Sm-*A*–Sm-*C* (or Sm-*C**) transition, the measured smectic layer spacing (d) shows a significant reduction in the first case and much smaller layer contraction in the second one [3]. For the purpose of our presentation, we will name the two models the "conventional Sm-*A*" and "de Vries-type Sm-*A*." Three experimental probes, namely, x-ray diffraction, ellipsometry, and calorimetry, were employed to gain better insight into the nature of the Sm-*A*–Sm-*C** transition of one compound showing almost no-layer-shrinkage behavior through the transition. Employing bulk sample cells, Lagerwall *et al.* [6] have studied this compound and acquired several important physical properties. Nevertheless, our higher-resolution measurements enable us to discover several critical features. Among them, our results indicate that upon cooling, there exists a crossover behavior from conventional Sm-*A* to de Vries-type Sm-*A*.

To obtain the high-resolution temperature variation of d near the Sm-*A*–Sm-*C** transition of 8422[2F3], we conducted detailed small angle x-ray diffraction from free-standing films using beam line X19A at National Synchrotron Light Source, Brookhaven National Laboratory. The molecular structure of 8422[2F3] is given at the top of Fig. 1. Bulk samples exhibit the following phase sequence: crystal (43.1°C) Sm-*C** (64.5°C) Sm-*A* (91°C) isotropic. The thick 8422[2F3] free-standing films were prepared inside a temperature regulated oven with temperature resolution better than 0.01 K. To minimize the attenuation of the x rays, the x-ray flight path and the film oven were filled with He gas. Excellent layer structures formed in free-standing films enable us to get very sharp (001) diffraction peaks. The x-ray wavelength was 5.016 Å. Although short at this wavelength, the penetration length of the x rays is, at least, equal to (or larger than) the thickness of the free-standing film (more than 500 layers). The contribution of the few interface-distorted surface layers to the diffraction is therefore negligible. To get the best experimental resolution, 0.07 mm input

*Present address: Advanced Photon Source, Argonne National Laboratory, Argonne, IL 60439, USA.

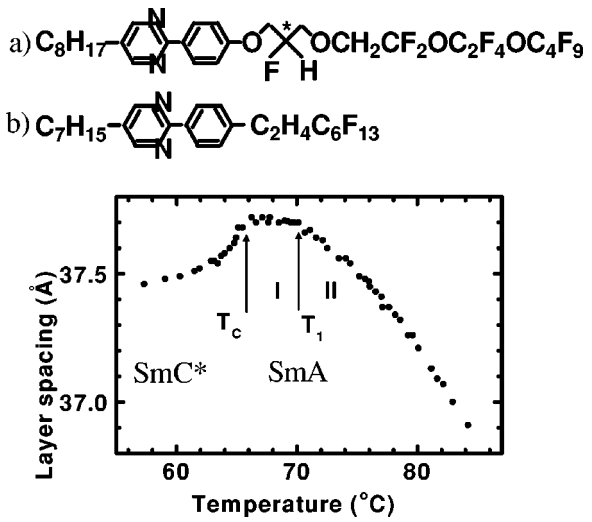

FIG. 1. The molecular structures of (a) 8422[2F3] and (b) FPP are shown at the top. The layer spacing as a function of temperature from a thick free-standing 8422[2F3] film. The Sm-A–Sm-C^* transition temperature (T_c) is denoted by the left arrow. The right arrow (T_1) separates the bulk Sm-A phase window into region I and II.

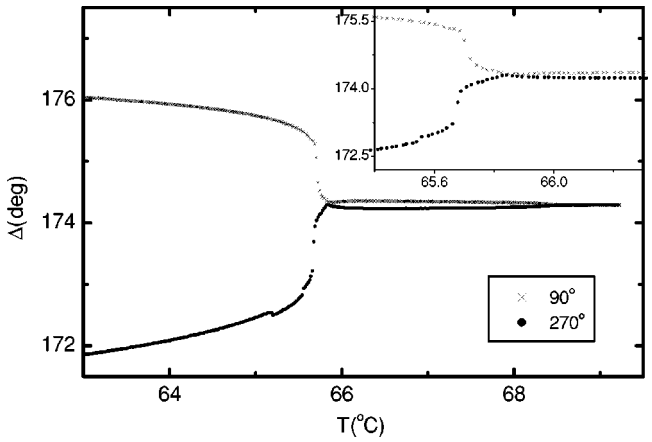

FIG. 2. Temperature dependence of Δ obtained upon cooling under two opposite directions of E (crosses, $a=90°$; dots, $a=270°$) from a 35-layer film. The inset shows details near the Sm-A–Sm-C^* transition.

and output vertical slits sizes were used to define the incident and diffracted beams. Each scan through the (001) Bragg peak was performed with a step size of 0.0005 Q_z. In addition, each Bragg peak was carefully optimized through θ and χ rocking scans at each peak position.

The full width at half maximum of the Bragg peaks remained at about 0.002 Q_z throughout the study. The measured d as a function of temperature is shown in Fig. 1 [8]. Upon cooling from the Sm-A phase, as usual, an increase in d is observed. At T_1 (about 4.5 K above the T_c), there exists an obvious slope change, and the temperature variation of d turns into a plateau before a small and smooth drop below T_c. Our high-resolution x-ray data reveal the first experimental observation of the existence of a conspicuous plateau just above T_c among various compounds showing no-layer-shrinkage behavior. The layer spacing only changes slightly ($\sim$0.2 Å) in the Sm-C^* temperature window shown, which corresponds to an $\approx$0.5 % change in layer spacing. In contrast, a conventional Sm-A compound usually exhibits about a 5 % change in the same temperature window. To facilitate further discussions, we will use regions I and II to denote these two different temperature windows above T_c, separated by T_1 as indicated in Fig. 1.

Employing null-transmission ellipsometry (NTE) [9,10], we have measured two ellipsometry parameters Ψ and Δ under various conditions, i.e., film thickness (N is number of layers), temperature, strength, or orientation (a) of the applied E field. Here Δ is the phase lag between the $\hat{p}$ and $\hat{s}$ components of the light incident upon the sample necessary to produce linearly polarized transmitted light after the free-standing film. The second parameter Ψ is the angle of the polarization of the transmitted light. Figure 2 displays Δ versus temperature obtained from a 35-layer film under two different E-field orientations ($a=90°$, Δ_{90} and 270°, Δ_{270}), which are perpendicular to the incident plane of the laser light. In region I, Δ_{90} is different from Δ_{270}. This indicates that the film is biaxial. Our detailed ellipsometric studies of this compound from thin free-standing films ($N<12$) indicate that the biaxiality is mainly due to the surface-enhanced molecular tilt [9]. In region II, the entire film is uniaxial. Just before the transition into the bulk Sm-C^* phase, Δ_{90} shows a dip while Δ_{270} exhibits a cusp. Similar temperature evolutions of Δ_{90} and Δ_{270} obtained from films of different thickness ($N<12$) allow us to unfold a new surface tilt profile in the Sm-C^* temperature range [9].

Three key physical parameters in simulating optical properties of free-standing films employing the 4×4 matrix method are d and two indices of refraction (n_o and n_e) in the principal molecular frame. Usually, we obtain these three parameters in the uniaxial Sm-A phase in which the ellipsometric parameters (Ψ and Δ) depend on d, N, the index of refraction along the layer normal $n_{\|}$, and the one within the layer plane $n_{\perp}$. By acquiring Ψ and Δ from a series of films (typically more than 50) of thickness from two to a few hundreds of layers, these important quantities can be determined by modeling the data using the uniaxial slab structure for the Sm-A phase.

At 70.2 °C, just above region I, we have spread 87 different 8422[2F3] films of various thicknesses, ranging from 2 to 247 layers, and acquired Ψ and Δ. Figure 3 shows the Ψ versus Δ plot as solid diamonds. The fact that N in free-standing films is quantized enables us to use the 4×4 matrix method to simulate all the data by choosing proper values of d, N, $n_{\|}$, and $n_{\perp}$. The simulated results shown as circles yield $n_{\perp}=1.401\pm0.001$, $n_{\|}=1.467\pm0.001$, and $d=3.77\pm0.04$ nm. Within our experimental resolution, the values of d determined from x-ray diffraction and NTE are in very good agreement. Similar measurements were conducted at 85 °C, a few degrees below the isotropic–Sm-A transition temperature and yielded $n_{\perp}=1.395\pm0.001$ which is only slightly smaller than the one obtained at 70.2 °C. To date, employing NTE, we have conducted detailed optical investigations of 12 liquid-crystal compounds showing conventional Sm-A behavior. Their average and standard deviation of two indices of refraction are $n_{\perp}=n_o=1.477\pm0.008$ and $n_{\|}=n_e$

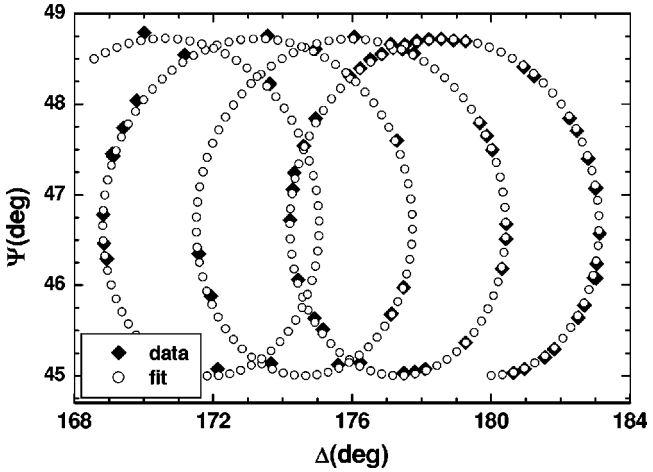

FIG. 3. Ψ vs Δ obtained at 70.2 °C from 87 films of 8422[2F3] compound (diamonds) along with fitted results (open circles).

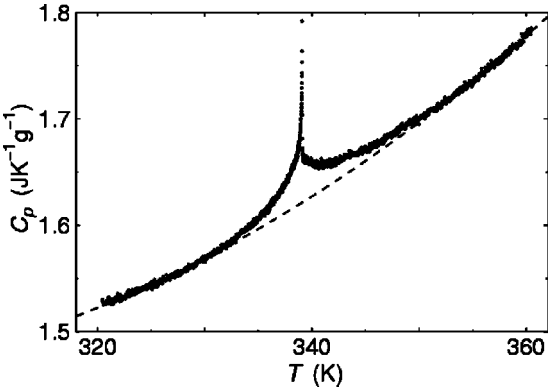

FIG. 4. Temperature dependence of heat capacity from 8422[2F3] sample. The data are acquired from the first cooling run. The dashed line shows the background contribution to the heat capacity.

$=1.617\pm0.031$ Their n_o values range from 1.452 to 1.497. If the diffuse-cone picture still held in the temperature region II for 8422[2F3], we would have obtained a value of $n_\perp$(within the layer plane) that is larger than n_o(determined in the molecular frame). To the contrary, our acquired value of $n_\perp$ for 8422[2F3] is much smaller than the n_o values of conventional Sm-*A* compounds. Once the surface-induced tilt layers set in within the region I, the films become biaxial and the above mentioned measurement technique is not applicable.

The small value of $n_\perp$ may be due to 8422[2F3] possessing one relatively long fluo-alkyl tail. In light of this observation, we have carried out similar measurements on another liquid-crystal compound, FPP, which has a long fluo-alkyl tail. Our measurements yielded $n_\perp=n_o=1.413\pm0.001$ which is again larger than that for 8422[2F3]. The molecular structure of FPP is given in Fig. 1 also.

Based on our x-ray and NTE results and the published results from electroclinic measurements [6], we propose the following scenario for the molecular packing in the Sm-*A* phase of 8422[2F3]. While in temperature region I, the de Vries Sm-*A* picture may be applicable, the conventional Sm-*A* arrangement prevails in temperature region II. There exists crossover behavior characterizing a change in molecular packing near T_1.

To further examine the Sm-*A*–Sm-C^* transition in this compound, heat capacity C_p has been measured with a high-resolution ultralow frequency ac calorimeter [11]. Hermetically sealed gold cells that contained about 10–20 mg of liquid-crystal sample were used. The temperature scan rate was about 0.03 K/h in the transition region. No detectable drift in the Sm-*A*–Sm-C^* transition temperature was observed, indicating the stability and high quality of the sample. After subtracting sample cell contributions, a typical temperature dependence of the C_p data is shown in Fig. 4. The dashed line in the figure shows the background heat capacity C_p (background), determined as a quadratic function of the temperature which joins the measured heat capacity data smoothly at temperatures away from T_c on both sides of the transition. In the vicinity of T_c, the heat capacity displays a large lambda-shape anomaly while no thermal signature can be detected near T_1. A significant feature is that the anomaly accompanying the transition is almost symmetric above and below T_c. A nonadiabatic scanning (NAS) mode measurement [12] has also been made, which revealed a latent heat at this transition, indicating that the transition is first order [13]. In accordance with this, an anomalous increase in the phase of the sample temperature response was observed in the ac mode measurement. Based on the following observations, the first-order nature of the transition is very weak. First, a significant pretransitional anomaly exists. Second, the latent heat observed in the NAS mode is small, being about 10 mJ/g, although this estimation is not so accurate due to the existence of a pretransitional anomaly showing almost divergent behavior. Third, the width of two-phase coexistence region observed in the ac mode is narrow, only about 16 mK.

The data of excess heat capacity C_p obtained by subtracting C_p (background) from C_p have been analyzed with the following renormalization-group expression [14]:

$$\Delta C_p = (A^\pm/\alpha)|t|^{-\alpha}(1 + D_1^\pm|t|^\zeta + D_2^\pm|t|) + B_c. \qquad (1)$$

Here $t=(T-T_c)/T_c$ and the superscript ± denote above and below T_c. Because the first-order nature of the transition is very weak, the use of Eq. (1) for the analysis of the present data is justified as a starting trial function. The exponent α was adjusted freely in the least-squares fitting procedure. The correction-to-scaling exponent ζ is dependent on the universality class, but has a theoretical value close to 0.5 [14], and therefore was fixed at 0.5 here. The result of the fitting is shown in Table I. Fits were made to the data over several ranges, and the maximum value of $|t|$ used in the fit, denoted as $|t|_{max}$, is shown in the table. For $|t|_{max}=0.001$ and 0.003, we see (a) the value is close to the tricritical value 0.5 and (b) the $D_1^\pm$ values are unusually large. The former point (a) is reasonable because the transition is very weakly first order and therefore close to a tricritical point that corresponds to a border between second- and first-order transitions. The latter point (b) is partly related to (a), and also to the first-order nature of the transition. Since the transition is first order, the critical constant term

TABLE I. Least-squares values of the adjustable parameters for fitting ΔC_p with Eq. (1). In the fits shown here, ζ has been fixed at 0.5, and $D_2^{\pm}$ have been fixed at zero. The units are $JK^{-1}g^{-1}$ for A^+ and B_c, and K for T_c.

$\lvert t\rvert_{max}$	T_c	α	$10^5 A^+$	A^-/A^+	D_1^+	D_1^-	B_c	χ_ν^2
0.001	339.103	0.54	1.95	19.60	1304	55	−0.025	1.00
0.003	339.104	0.52	0.84	51.5	11 210	205	−0.170	1.11
0.01	339.083	0.32	13.2	8.83	−267	−42	0.067	1.74

B_c need not be equal above and below T_c. This implies an existence of a gap ΔB_c at T_c, which is accounted for by the first-order correction term, behaving almost a constant term when $\alpha \approx 0.5$ and $\zeta \approx 0.5$. Allowing B_c to be different for above and below T_c and omitting the D_1 term yielded adequate fits for small $\lvert t\rvert_{max}$. For $\lvert t\rvert_{max}=0.01$, however, the inclusion of the D_2 term was necessary with unacceptably large values $D_2^{\pm}=10^3$. This suggests that the deviation from the asymptotic critical behavior away from T_c is not explained as corrections to the scaling, but rather a manifestation of a different critical behavior. Further data analysis is in progress.

Three experimental probes have been used to obtain essential information related to NLS behavior of 8422[2F3]. Both x-ray diffraction and ellipsometry results indicate the existence of crossover behavior near T_1 from a conventional Sm-*A* molecular packing to a de Vries Sm-*A* one. Near T_1, the sample does not show any thermal signature under our high-resolution calorimetric studies. Meanwhile, our calorimetric results reveal that the Sm-*A*–Sm-C^* transition is weakly first order. According to their electro-optical investigations, the de Vries compound reported by Clark *et al.* has a first-order Sm-*A*–Sm-C^* transition [5].

We are grateful to Professor P. Barois for his help and to Professor T. Lubensky for helpful discussions. This work was partially supported by the National Science Foundation under Grant No. DMR-0106122, a Grant-in-Aid for Scientific Research from the Ministry of Education and Science of Japan, Grant No. 12129204, and the Donors of the Petroleum Research Fund, administered by the American Chemistry Society. The research was carried out in part at the National Synchrotron Light Source, Brookhaven National Laboratory, which is supported by the U.S. Department of Energy, Division of Materials Sciences and Division of Chemical Sciences, under Contract No. DE-AC02-98CH10886. X.F.H. acknowledges financial support from the Stanwood Johnston Memorial Foundation at the University of Minnesota. The liquid-crystal compound was kindly provided by 3M Company, St. Paul, Minnesota.

[1] R. B. Meyer, L. Liebert, L. Strzelecki, and P. Keller, J. Phys. (Paris) **36**, L69 (1975).
[2] S. Garoff and R. B. Meyer, Phys. Rev. Lett. **38**, 848 (1977).
[3] M. S. Spector, P. A. Heiney, J. Naciri, B. T. Weslowski, D. B. Holt, and R. Shashidhar, Phys. Rev. E **61**, 1579 (2000).
[4] J. V. Selinger, P. J. Collings, and R. Shashidhar, Phys. Rev. E **64**, 061705 (2001).
[5] N. A. Clark, T. Bellini, R. F. Shao, D. Coleman, S. Bardon, D. R. Link, X. H. Chen, M. D. Wand, D. M. Walba, P. Rudquist, and S. T. Lagerwall, Appl. Phys. Lett. **80**, 4097 (2002).
[6] J. P. F. Lagerwall, F. Giesselmann, and M. D. Radcliffe, Phys. Rev. E **66**, 031703 (2002).
[7] A. de Vries, A. Ekachai, and N. Spielberg, Mol. Cryst. Liq. Cryst. **49**, 143 (1979); A. de Vries, *ibid.* **49**, 179 (1979).
[8] In contrast to our measured layer spacing $d=3.77$ nm at T_c, Lagerwall *et al.* [6] reported $d=3.87$ nm at T_c.
[9] X. F. Han, S. T. Wang, A. Cady, M. D. Radcliffe, and C. C. Huang, Phys. Rev. Lett. **91**, 045501 (2003).
[10] R. M. A. Azzam and N. M. Bashara, *Ellipsometry and Polarized Light* (North-Holland, Amsterdam, 1989).
[11] K. Ema and H. Yao, Thermochim. Acta **304/305**, 157 (1997).
[12] H. Yao, K. Ema, and C. W. Garland, Rev. Sci. Instrum. **69**, 172 (1998).
[13] Employing DSC measurements, Lagerwall *et al.* [6] have concluded that the Sm-*A*–Sm-C^* transition of this compound is continuous.
[14] C. Bagnuls and C. Bervillier, Phys. Rev. B **32**, 7209 (1985).